Available online at www.sciencedirect.com
ScienceDirect
C. R. Mecanique 334 (2006) 593–598
COMPTES RENDUS MECANIQUE
http://france.elsevier.com/direct/CRAS2B/

Effects of conductivity jumps in the envelope of a kinematic dynamo flow

Raphael Laguerre [a,d,*], Caroline Nore [a,b], Jacques Léorat [c], Jean-Luc Guermond [a,d]

[a] *LIMSI-CNRS, BP 133, 91403 Orsay cedex, France*
[b] *Université Paris XI, département de physique, 91405 Orsay cedex, France*
[c] *LUTH, observatoire de Paris-Meudon, 92195 Meudon, France*
[d] *Department of Mathematics, Texas A&M University, 3368 Tamu, College Station, TX 77843-3368, USA*

Received 8 June 2006; accepted 27 June 2006

Available online 12 September 2006

Presented by René Moreau

Abstract

This Note reports on numerical simulations of the kinematic dynamo action in a test flow modeling the Von Kármán Sodium (VKS) experiment performed at CEA-Cadarache. We show that the conductivity of the vessel greatly influences the critical magnetic Reynolds number. These effects are dramatically amplified as the ratio of the conductivity of the vessel to that of the sodium increases from 1 to 5. ***To cite this article: R. Laguerre et al., C. R. Mecanique 334 (2006).***

Résumé

Influence des discontinuités de conductivité dans l'enveloppe de l'écoulement d'une dynamo cinématique. Cette Note présente de nouveaux résultats sur l'influence de couches de conducteur sur le seuil de l'instabilité dynamo dans un écoulement simulant l'expérience Von Kármán Sodium (VKS) menée au CEA-Cadarache. Nous montrons que les effets d'une enveloppe statique sur le seuil d'instabilité sont amplifiés lorsque le rapport de conductivité de l'enveloppe sur celle du sodium passe de 1 à 5. ***Pour citer cet article : R. Laguerre et al., C. R. Mecanique 334 (2006).***

Keywords: Computational fluid mechanics; Instability; Kinematic dynamo

Mots-clés : Mécanique des fluides numériques ; Instabilité ; Dynamo cinématique

Version française abrégée

Les dynamos expérimentales au sodium liquide en cours de développement utilisent des containeurs métalliques dont la conductivité est supérieure à celle du sodium. L'objet de cette Note est de montrer que l'épaisseur et le rapport

* Corresponding author.
E-mail addresses: laguerre@limsi.fr (R. Laguerre), nore@limsi.fr (C. Nore), jacques.leorat@obspm.fr (J. Léorat), guermond@math.tamu.edu (J.-L. Guermond).

1631-0721/$ – see front matter
doi:10.1016/j.crme.2006.06.008

de conductivité de l'enveloppe métallique sur celle du sodium ont des effets très importants sur le nombre de Reynolds magnétique critique de déclenchement de l'instabilité dynamo. Nos simulations numériques dans des configurations proches de l'expérience VKS de Cadarache montrent que le saut de conductivité est favorable en présence d'une enveloppe latérale, mais est défavorable en présence de couvercles (voir Tableau 1). Une interprétation physique est proposée pour comparer trois cas typiques. Cet effet de conductivité d'enveloppe pourrait affecter les performances des dynamos fluides expérimentales en cours d'étude.

1. Introduction

The Earth's magnetic field is generated by the so-called dynamo effect. Two experiments have successfully reproduced this phenomenon in laboratories so far [1,2]. The first experiment is based on a helical flow in a vertical pipe (Ponomarenko's flow) and generates a time-dependent magnetic field when the magnetic Reynolds number $R_m = \mu\sigma LV$ is larger than the dynamo threshold R_m^c (here μ is the magnetic diffusivity of the fluid, σ the conductivity, and L, V are typical length and velocity scales). In the second experiment, the flow is divided into several cells where a helical flow is maintained (Robert's flow) and gives rise to a stationary magnetic field above criticality.

Among other recent experiments, the Von Kármán Sodium (VKS) experiment seems promising. This experiment is based on a flow generated by two counter-rotating impellers located at the top and bottom of a cylindrical vessel. In the counter-rotating regime, the flow is divided into two toroidal cells by an azimuthal shear layer in the median plane. In each cell, the rotating disk acts as a centrifugal pump and mass conservation yields a recirculation. For more details on the flow, see [3] in laminar regime and [4] in turbulent regime. No dynamo action was observed in the first experimental device (VKS1), where the maximum achievable magnetic Reynolds number was below the threshold calculated in [5]. The optimization of the previous device has led to a second set-up (VKS2) which is currently tested.

Numerical simulations on VKS2-like set-ups have been carried out in [4,7] to evaluate the influence of the thickness of the vessel containing the sodium. Due to methodological reasons, in these computations the ratio of the conductivity of the vessel to that of the fluid is assumed to be 1, which is not realistic. It has been shown in [4,7] that accounting for the thickness of the side walls of the vessel (see case S in Fig. 3) decreases the critical magnetic Reynolds number. It has also been shown that accounting for the thickness of the bottom and top lids of the vessel (see case SL in Fig. 3) increases the critical magnetic Reynolds number. A small decrease in R_m^c is crucial from the experimental point of view, since the power needed in the experiment scales like $\mathcal{O}(R_m^3)$. These results have led us to redo the computations with a more realistic copper vessel, with conductivity ratio $\sigma_{\text{copper}}/\sigma_{\text{sodium}} \simeq 5$, using a new finite element code that we recently developed to account for discontinuous conductivities. The purpose of this Note is to report our findings.

2. Overview of the approximation method

In this section we give a brief overview of the numerical method which is used. The problem is modeled by the MHD equations in the eddy current approximation with no retroaction of the magnetic field on the velocity field (kinematic dynamo approximation):

$$\mu\partial_t \mathbf{H} = -\nabla\times\mathbf{E}; \quad \nabla\times\mathbf{H} = \sigma(\mathbf{E}+\mathbf{u}\times\mu\mathbf{H}), \text{ boundary and initial data } \mathbf{E}\times\mathbf{n}|_\Gamma = \mathbf{a}; \quad \mathbf{H}|_{t=0} = \mathbf{H}_0 \tag{1}$$

where $\mathbf{H}$ is the magnetic field, $\mathbf{E}$ the electric field, $\mathbf{u}$ an imposed velocity field, σ the electric conductivity, μ the magnetic permeability, and Γ is the boundary of the computational domain. This system is solved in a heterogeneous domain composed of conducting regions of different conductivities ($\sigma_1 > 0,\ \sigma_2 > 0,\ \ldots$) and an insulating region (vacuum, $\sigma_0 = 0$). Since the magnetic field is curl free in vacuum, it can be expressed as the gradient of a scalar potential ϕ, as long as the insulating domain is simply connected. $\mathbf{E}$ can then be eliminated and (1) can be re-written in term of $\mathbf{H}$ and ϕ only. Enforcing continuity of $\mathbf{H}$ and $\nabla\phi$ across interfaces is a significant numerical difficulty. In our Finite Element approximation, continuity is not enforced in the function spaces as in [8], where Nédélec elements are used, but is rather weakly imposed using an Interior Penalty Galerkin method (IPG) together with Lagrange elements. This method has been shown to be stable and convergent in [9,10].

Since the geometry is axisymmetric, the equations are written in cylindrical coordinates and the approximate solution is expanded in Fourier series in the azimuthal direction and nodal Lagrange finite elements in the meridian plane. The magnetic field is approximated using piecewise linear elements and the scalar potential is approximated using piecewise quadratic elements. The time is discretized by means of a semi-implicit Backward Finite Difference

method of second order (BDF2). At the boundary of the computational domain, we can impose Robin, Neumann, or Dirichlet boundary conditions on ϕ.

The computations reported hereafter are carried out with the following discretization characteristics: the conducting domain, composed of a finite cylinder (fluid) and an additional external layer (vessel), is discretized using a quasi-uniform grid of meshsize $\delta_x = 1/40$. The conducting region is embedded in a spherical insulating domain of radius 10 whose meshsize varies from $\delta_x = 1/40$ at the inner interface to $\delta_x = 1$ at the outer boundary of the sphere. The fluid flow is modeled by the following so-called MND velocity field [6] expressed in cylindrical coordinates (r, z, θ): for $0 \leqslant r \leqslant 1$ and $-1 \leqslant z \leqslant 1$:

$$v_r = -\frac{\pi}{2} r(1-r)^2(1+2r)\cos(\pi z); \quad v_\theta = 4\varepsilon r(1-r)\sin\left(\frac{\pi}{2}z\right); \quad v_z = (1-r)\left(1+r-5r^2\right)\sin(\pi z) \tag{2}$$

The parameter ε is the toroidal to poloidal flow ratio. We use $\varepsilon = 0.7259$ which yields near optimal dynamo action, as shown in [6]. Since the flow is axisymmetric, the magnetic azimuthal modes evolve independently; as a result, we restrict ourselves to the azimuthal mode 1 which is the most unstable. Hereafter, we use the following definition of the magnetic Reynolds number: $R_m = \mu\sigma_{\text{fluid}} r_0 v_{\max}$, where r_0 is the radius of the inner cylinder and $v_{\max}$ the maximum of the velocity. The vessel containing the fluid is a hollow cylinder (see Fig. 3). The nondimensional thickness of the side wall is denoted by w and that of the top and bottom lids is denoted by l. The conductivity ratio $\sigma_{\text{vessel}}/\sigma_{\text{fluid}}$ is denoted by X.

3. Case 1: influence of conducting annuli

We first consider a vessel having the shape of cylindrical annulus, i.e., the thickness of the lids l is assumed to be infinitely thin ($l = 0$) (see case S in Fig. 3). Two cases are considered: $w = 1$ and $w = 0$ (no annulus). When the conductivities of the fluid and the vessel are identical, $X = 1$, our code predicts critical magnetic Reynolds numbers that agree with previous studies [4,7] whether $w = 0$ or $w = 1$. In Fig. 1(a) we compare the magnetic field growth rates γ_H for the cases ($w = 0$), ($w = 1$, $X = 1$) and ($w = 1$, $X = 5$). When there is no conductivity jump, $R_m^c = 63.5 \pm 0.5$ for $w = 0$ and $R_m^c = 45 \pm 0.5$ for $w = 1$. When $X = 5$, the critical magnetic Reynolds number decreases to $R_m^c = 40 \pm 0.5$ for $w = 1$. These results confirm that adding a conducting annulus lowers R_m^c as already shown in [11,12,4,7]. The novelty that we emphasize in this Note is that increasing the conductivity of the annulus significantly amplifies this effect. This result points in the same direction as those obtained by Dobler et al. [13] for the Ponomarenko dynamo. Note however that when $w = 1$, the growth rate for $X = 5$ becomes smaller than that for $X = 1$ when $R_m \geqslant 50$.

Fig. 1(b) shows $R_m^c(w)$ as a function of w for $X = 1$ and $X = 5$. We observe that R_m^c decreases quasi-exponentially with respect to w at $X = 1$ with the typical lengthscale 0.2, thus confirming results from [4], then R_m^c reaches an asymptote for large w. In order to analyze the impact of a conducting annulus w on R_m^c, we consider the energy balance:

$$\frac{1}{2}\frac{\mathrm{d}}{\mathrm{d}t}E = [R_m P - D]E$$

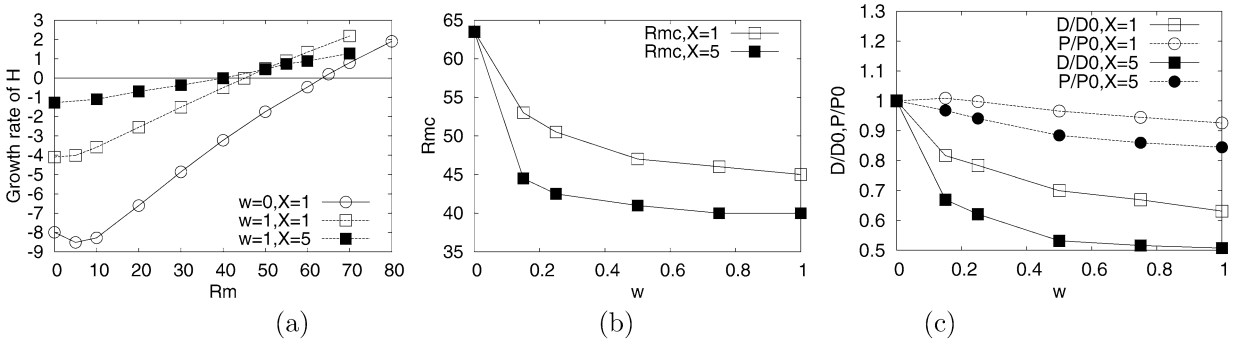

Fig. 1. (a) Growth rates γ_H for annuli of characteristics ($w = 0$), ($w = 1$, $X = 1$), ($w = 1$, $X = 5$). (b) Critical magnetic Reynolds number R_m^c as a function of w, for $X = 1$ and $X = 5$. (c) Ratios D/D_0 and P/P_0 for $X = 1$ and $X = 5$.

where, upon denoting by Ω_c^i the conducting domain of conductivity σ_i and by Ω the computational domain, the total energy is

$$E = \int_{\Omega} \mathbf{H}^2$$

the nondimensionalized dissipation is

$$D = E^{-1}\left\{\sum_i X_i^{-1} \int_{\Omega_c^i} [\nabla \times \mathbf{H}]^2\right\}$$

and the nondimensionalized production is

$$P = E^{-1} \int_{\Omega_c^{\text{fluid}}} \big[\mathbf{H} \times (\nabla \times \mathbf{H})\big] \cdot \mathbf{U}$$

This balance can be rewritten as: $\gamma_H = R_m P - D$ where γ_H, P, and D depend on R_m and w (and l with lid layers, see next section). At criticality ($\gamma_H^c = 0$), we have verified that

$$R_m^c(w) = D\big(R_m^c(w), w\big)/P\big(R_m^c(w), w\big)$$

for all w. Upon denoting by D_0 and P_0 the value of D and P at $w = 0$, $l = 0$, and $R_m = R_m^c(0)$, it is interesting to study the variation of the normalized dissipation $D(R_m^c(w), w)/D_0$ and production $P(R_m^c(w), w)/P_0$ with respect to w. For both values of $X = 1$ and $X = 5$, the ratio

$$R_m^c(w)/R_m^c(0) = [D/D_0]/[P/P_0]$$

is driven more by the decrease of D/D_0 than by that of P/P_0 when w increases.

4. Case 2: influence of conducting top and bottom lids

We now set the thickness of the annulus to $w = 0.5$, and we analyze the effect of top and bottom lids of thickness l. This case has been studied in [7] with no conductivity jump, i.e., $X = 1$, the main result being that R_m^c dramatically increases with respect to l. We display in Fig. 2(a) $R_m^c(w = 0.5, l)$ as a function of l for $X = 1$ and $X = 5$. For $X = 1$, our results differ from those of Stefani et al. [7] by 10%; this might be explained by the difference in resolutions used in the two numerical methods. We observe that R_m^c increases with l and that this effect is again amplified by the conductivity jump, the variation being the largest in the range $0 \leqslant l \leqslant 0.2$. We display in Fig. 2(b) the normalized dissipation and production terms $D(R_m^c(w = 0.5, l), l)/D_0$ and $P(R_m^c(w = 0.5, l), l)/P_0$ as functions of l, where D_0 and P_0 denote the values of $D(R_m^c(w = 0.5, l), l)$ and $P(R_m^c(w = 0.5, l), l)$ at $l = 0$ (note that D_0 and P_0 depend on X). For both values of X, the ratio $R_m^c(w = 0.5, l)/R_m^c(w = 0.5, 0) = [D/D_0]/[P/P_0]$ is driven more by the increase of D/D_0 than by that of P/P_0 when l increases. When computing the total dissipation and the partial dissipations induced by each component of the current for $X = 5$ as a function of l (data not shown), we have observed that the dissipation is dominated by its azimuthal and radial components, which suggests that strong azimuthal and radial currents are generated (see discussion below).

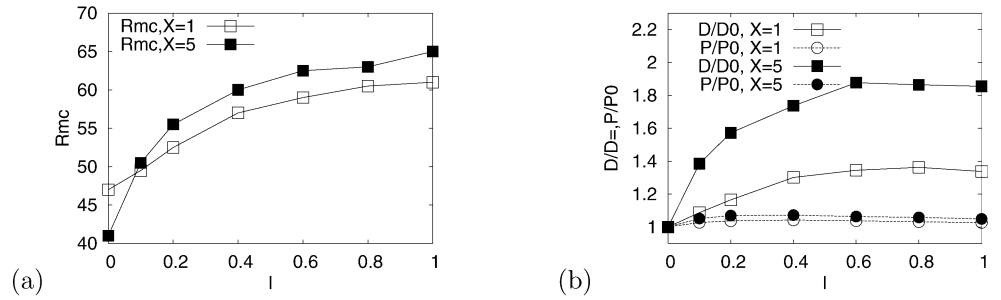

Fig. 2. (a) R_m^c as functions of l, for $X = 1$ and $X = 5$ ($w = 0.5$). (b) Ratios $D(R_m^c(w = 0.5, l), l)/D_0$ and $P(R_m^c(w = 0.5, l), l)/P_0$ for $X = 1$ and $X = 5$ as indicated.

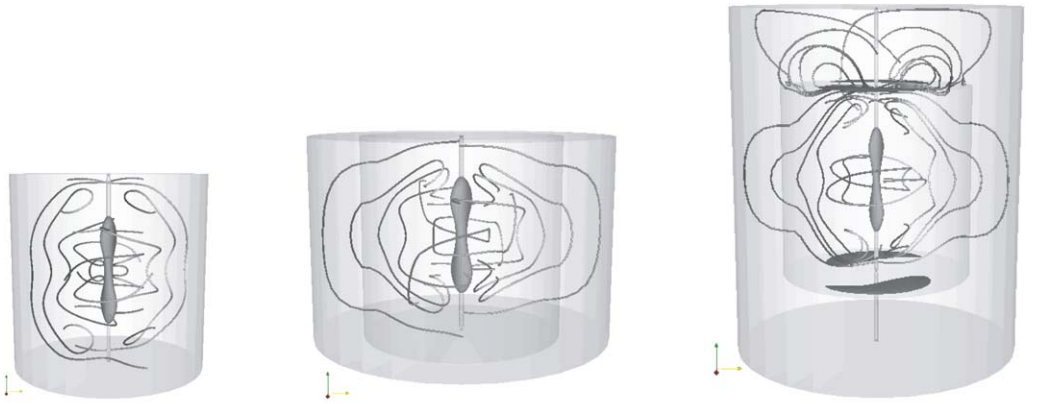

Fig. 3. Isosurface of 50% of the total dissipation and current lines for (Case N) $X = 5$, $w = 0$, $l = 0$ and $R_m = 65 > R_m^c = 63.5$ (Case S) $X = 5$, $w = 0.5$, $l = 0$ and $R_m = 42 > R_m^c = 41$ (Case SL) $X = 5$, $w = 0.5$, $l = 0.8$ and $R_m = 65 > R_m^c = 63$.

Table 1
Critical magnetic Reynolds numbers R_m^c for different geometries and conductivities

	$w = 0,\ l = 0$	$w = 1,\ l = 0$	$w = 0.5,\ l = 0$	$w = 0.5,\ l = 1$
$X = 1$	63.5	45	47	61
$X = 5$	63.5	40	41	65

5. Interpretation and conclusions

To better understand the behavior of R_m^c with respect to w and l, we now compare the spatial distribution of dissipation and currents in three typical cases (see also [7]). The cases considered are (i) case N: no envelope; (ii) case S: an annulus of thickness $w = 0.5$ with $X = 5$ and no lids $l = 0$; (iii) case SL: an annulus of thickness $w = 0.5$ and two lids of thickness $l = 0.8$ with $X = 5$. The results are reported in Fig. 3. For the cases N and S, most of the dissipation is concentrated in the fluid, close to the cylinder axis, whereas in the SL case, new dissipation patterns occur within the lids. The figure shows some characteristic lines of the current vector field. The spatial distribution of the lines close to the axis is pretty similar in the three cases, but it significantly differs in regions close to the envelope. Going from the case N to the case S, the currents formerly constrained in the flow volume are deformed and expand to fill the annulus on large scales, suggesting that the dissipation decreases as indeed observed. Going from the case S to the case SL, additional current loops at small scales appear within the top and bottom lids leading to more Ohmic dissipation. The decrease of dissipation when going from the case N to the case S is compatible with the observations of Avalos and Plunian [12] made on the Karlsruhe dynamo.

Although a predictive explanation of the variation of the dynamo threshold is still lacking at the present time, the impact of an envelope seems crucial for the design of experimental fluid dynamos. The increase of R_m^c from the S to the SL configuration suggests to diminish the influence of the lid by lowering its conductivity. In the near future, we plan to optimize the geometry of the envelope of the VKS set-up by using the experimental mean flow [4] and the actual sizes and conductivities of the materials that are used (sodium, copper, stainless steel).

The main results of this Note are summarized in Table 1. An annulus of characteristics ($w = 0.5,\ l = 0$) decreases R_m^c by 26% when the conductivity is uniform, $X = 1$, and by 35% when the conductivity ratio is $X = 5$. In contrast, adding a lid, $l = 1$, to the annulus, $w = 0.5$, increases R_m^c by 30% when the conductivity is uniform and by 59% when the conductivity ratio is $X = 5$.

Acknowledgement

Fruitful discussions with F. Stefani are acknowledged.

References

[1] A. Gailitis, et al., Detection of a flow induced magnetic field eigenmode in the Riga dynamo facility, Phys. Rev. Lett. 84 (2000) 4365.
[2] R. Stieglitz, U. Müller, Experimental demonstration of a homogeneous two-scale dynamo, Phys. Fluids 13 (2001) 561.
[3] C. Nore, M. Tartar, O. Daube, L.S. Tuckerman, Survey of instability thresholds of flow between exactly counter-rotating disks, J. Fluid Mech. 511 (2004) 45–65.
[4] F. Ravelet, A. Chiffaudel, F. Daviaud, J. Léorat, Towards an experimental von Kármán dynamo: numerical studies for an optimized design, Phys. Fluids 17 (2005) 117104.
[5] L. Marié, J. Burguete, F. Daviaud, J. Léorat, Numerical study of homogeneous dynamo based on experimental von Kármán type flows, Eur. Phys. J. B 33 (2003) 469.
[6] L. Marié, C. Normand, F. Daviaud, Galerkin analysis of kinematic dynamos in the von Kármán geometry, Phys. Fluids 18 (2006) 017102.
[7] F. Stefani, M. Xu, G. Gerbeth, F. Ravelet, A. Chiffaudel, F. Daviaud, J. Léorat, Ambivalent effects of added layers on steady kinematic dynamos in cylindrical geometry: application to the VKS experiment, Eur. J. Mech. B Fluid (2006), in press.
[8] A. Bossavit, Electromagnétisme en vue de la modélisation, SMAI/Springer-Verlag, Paris, 1993.
[9] J.-L. Guermond, R. Laguerre, J. Léorat, C. Nore, An Interior Penalty Galerkin Method for the MHD equations in heterogeneous domains, J. Comput. Phys. (2006), in press.
[10] R. Laguerre, C. Nore, J. Léorat, J.-L. Guermond, Induction effects in isolated axisymmetric conductors using a new finite element method, in: D. Carati, B. Knaepen (Eds.), Proceedings MHD Summer Program, 2006.
[11] R. Kaiser, A. Tilgner, Kinematic dynamos surrounded by a stationary conductor, Phys. Rev. E 60 (1999) 2949.
[12] R. Avalos-Zuniga, F. Plunian, A. Gailitis, Influence of electromagnetic boundary conditions onto the onset of dynamo action in laboratory experiments, Phys. Rev. E 68 (2003) 066307.
[13] W. Dobler, P. Frick, R. Stepanov, Screw dynamo in a time-dependent pipe flow, Phys. Rev. E 67 (2003) 056309.